Vol. 542: 13–24, 2016
doi: 10.3354/meps11571

MARINE ECOLOGY PROGRESS SERIES
Mar Ecol Prog Ser

Published January 19

Isotopic niche variability in macroconsumers of the East Scotia Ridge (Southern Ocean) hydrothermal vents: What more can we learn from an ellipse?

W. D. K. Reid[1,*], C. J. Sweeting[2], B. D. Wigham[3], R. A. R. McGill[4], N. V. C. Polunin[5]

[1]Ridley Building, School of Biology, Newcastle University, Newcastle, NE1 7RU, UK
[2]Marine Management Organisation, Lancaster House, Hampshire Court, Newcastle upon Tyne, NE4 7YH, UK
[3]Dove Marine Laboratory, School of Marine Science & Technology, Newcastle University, Cullercoats, NE30 4PZ, UK
[4]NERC Life Sciences Mass Spectrometry Facility, Scottish Universities Environmental Research Centre, East Kilbride, G75 0QF, UK
[5]Ridley Building, School of Marine Science & Technology, Newcastle University, Newcastle, NE1 7RU, UK

ABSTRACT: Aspects of between-individual trophic niche width can be explored through the isotopic niche concept. In many cases isotopic variability can be influenced by the scale of sampling and biological characteristics including body size or sex. Sample size-corrected (SEAc) and Bayesian (SEAb) standard ellipse areas and generalised least squares (GLS) models were used to explore the spatial variability of $\delta^{13}C$ and $\delta^{15}N$ in *Kiwa tyleri* (decapod), *Gigantopelta chessoia* (peltospirid gastropod) and *Vulcanolepas scotiaensis* (stalked barnacle) collected from 3 hydrothermal vent field sites (E2, E9N and E9S) on the East Scotia Ridge (ESR), Southern Ocean. SEAb only revealed spatial differences in isotopic niche area in male *K. tyleri*. However, the parameters used to draw the SEAc, eccentricity (*E*) and angle of the major SEAc axis to the *x*-axis (θ), indicated spatial differences in the relationships between $\delta^{13}C$ and $\delta^{15}N$ in all 3 species. The GLS models indicated that there were spatial differences in isotope–length trends, which were related to *E* and θ of the SEAc. This indicated that *E* and θ were potentially driven by underlying trophic and biological processes that varied with body size. Examination of the isotopic niches using standard ellipse areas and their parameters in conjunction with length-based analyses provided a means by which a proportion of the isotopic variability within each species could be described. We suggest that the parameters *E* and θ offer additional ecological insight that has so far been overlooked in isotopic niche studies.

KEY WORDS: Trophic niche width · Carbon fixation · Size · Epibionts · Endosymbiosis

INTRODUCTION

Hutchinson's definition of the ecological niche as a 'n-dimensional hypervolume' encompassing all the environmental factors that allow a species to inhabit a given area (Hutchinson 1957) encapsulates a huge amount of ecological complexity that is challenging to parameterise. More tractable are subsets of the ecological niche such as the trophic niche, which examines prey diversity and nutritional resources (Peterson et al. 2011). For many species, diet and habitat will change through life, resulting in ontogenetic changes within niche space (Werner & Gilliam 1984), which may not be consistent spatially or between sexes (Ramirez-Llodra et al. 2000, Forero et al. 2002, Marsh et al. 2015). Examining the breadth of nutritional resources a species exploits as it grows has important ecological consequences for understanding natural selection and species' adaptation and resilience to natural or anthropogenic perturbation (Bolnick et al. 2003, Wiens & Graham 2005, Layman et al. 2007b).

*Corresponding author: william.reid@newcastle.ac.uk

Publisher: Inter-Research · www.int-res.com

Stable isotope analysis is a tool for investigating intraspecific trophic niche variation (Bolnick et al. 2003, Bearhop et al. 2004, Sweeting et al. 2005) that has advantages over conventional techniques such as stomach content analysis and behavioural observations. Carbon (^{13}C:^{12}C expressed as $\delta^{13}C$) and nitrogen (^{15}N:^{14}N expressed as $\delta^{15}N$) stable isotope data provide a time-integrated signal of the materials assimilated from an individual's diet (Hesslein et al. 1993, Martinez del Rio et al. 2009) rather than providing a snap-shot of what an individual has consumed (Pinnegar & Polunin 1999). Trophic discrimination also results in consumers being 0 to 1.5‰ enriched in ^{13}C and 2.3 to 5‰ enriched in ^{15}N relative to their food source (Caut et al. 2009), allowing $\delta^{13}C$ to be used to identify sources of primary production and $\delta^{15}N$ to assess relative trophic position (Post 2002). Furthermore, $\delta^{13}C$ and $\delta^{15}N$ values often provide spatial-integrated signals when consumers move amongst habitats with different isotopic baselines (McMahon et al. 2013).

The isotopic niche reflects what an animal assimilates from its diet and the habitat in which it resides (Bearhop et al. 2004, Newsome et al. 2007) and is thus an approximation of the trophic niche (Jackson et al. 2011). Many species undertake ontogenetic or body size changes in habitat use or diet as a result of energetic and nutritional demands (Werner & Gilliam 1984), which are captured by their $\delta^{13}C$ and $\delta^{15}N$ values. The isotopic variability described by the isotopic niche represents the between-individual component (i.e. among-individual variation in resource use or physiological response to the environment) of the trophic niche (Bolnick et al. 2003, Jackson et al. 2011, Deudero et al. 2014, Dubois & Colombo 2014). The isotopic niche is often visualised as bivariate plots of mean $\delta^{13}C$ and $\delta^{15}N$ values and variance estimates (Bearhop et al. 2004). Statistical methods examining the dispersion of stable isotope values in *xy*-space (Layman et al. 2007a, Turner et al. 2010, Jackson et al. 2011) include convex hull (Layman et al. 2007a) and standard ellipse area (SEA) (Jackson et al. 2011); these aim to define a species' trophic niche in isotopic-space with each data point representing an individual's use of resources and habitat (Layman et al. 2012).

SEA appears to offer greater flexibility than convex hull area as it is more robust to differences in sample sizes (Jackson et al. 2011, Syväranta et al. 2013) and allows areas to be compared by Bayesian inference (Jackson et al. 2011). The parameters used to calculate and plot the SEA include: the lengths of the semi-major (*a*) and semi-minor (*b*) axes of the SEA; the angle in radians (θ) between *a* and the *x*-axis; the eccentricity (*E*) of the standard ellipse between $0 < E < 1$, where $E = 0$ is a perfect circle and $E \rightarrow 1$ indicates the standard ellipse becomes more elongated (Jackson et al. 2011, Parnell & Jackson 2011). Turner et al. (2010) originally proposed the use of *E* as a measure of isotopic variability. However, *E* and θ have not been reported to date in relation to SEA and may help inform its ecological interpretation. *E* and θ, therefore, may have the potential to distinguish isotopic niche areas, which are similar in size, but the relationship between $\delta^{13}C$ and $\delta^{15}N$ among locations or species are obviously different. This may lead a researcher to address follow-up questions: Is variation in the major axis random, or can it be described by an unidentified grouping variable, e.g. size, sex or site?

In this study, we address the question: What more can we learn from an ellipse? The focus here is expanding the potential of SEA by incorporating *E* and θ into an assessment of isotopic variability using fauna collected from deep-sea hydrothermal vents. Hydrothermal vents are chemically reducing habitats distinct from the surrounding deep sea. They exhibit strong inter- and intraspecific (e.g. body size and sex) zonation in relation to localised geochemical environmental gradients that occur over metres (Podowski et al. 2010, Marsh et al. 2012). The result is many hydrothermal vent fauna exhibit a great deal of isotopic variability among and within species (Colaco et al. 2002, De Busserolles et al. 2009, Reid et al. 2013), making hydrothermal vent fauna interesting species to examine trophic niche concepts.

Specifically, $\delta^{13}C$ and $\delta^{15}N$ were used to determine whether the intraspecific isotopic variability differed among sampling sites with different vent fluid chemistry and to what extent this variability was a function of individual length and/or sex. The visually dominant macroconsumers *Kiwa tyleri* (decapod) (Thatje et al. 2015), *Vulcanolepas scotianesis* (stalked barnacle) (Buckeridge et al. 2013) and *Gigantopelta chessoia* (gastropod) (Chen et al. 2015) are found at East Scotia Ridge (ESR) hydrothermal vents and potentially represent grazing, suspension feeding and endosymbiotic trophic guilds, respectively (Marsh et al. 2012, Rogers et al. 2012). The objectives were to: (1) compare isotopic niches among sites and between sexes; (2) assess whether SEA parameters *E* and θ might provide additional information to distinguish SEA with similar areas; and (3) examine whether regional differences in isotopic niche areas could be described by relationships between $\delta^{13}C$ or $\delta^{15}N$ and sex or length.

MATERIALS AND METHODS

Study sites, collection and sample processing

Samples were collected from on board the RRS 'James Cook' during the 2010 austral summer (7 January to 21 February) using the remotely operated vehicle (ROV) 'Isis' at hydrothermal vent fields on the E2 and E9 ridge segments of the East Scotia Ridge, Southern Ocean (Fig. 1). The E2 and E9 vent fields are situated ~440 km apart at 56° 05.35′ S, 30° 19.20′ W and 60° 02.50′ S, 29° 58.93′ W, at depths of ~2600 and ~2400 m and contain high temperature venting >300°C. The end-member fluid chemistry and chimney mineralisation differed between vent fields and also between the northern (E9N) and southern (E9S) sections of E9 (James et al. 2014). Ambient seabed water temperatures were 0.0°C at E2 and between −0.1°C and −1.3°C at E9 (Rogers et al. 2012). Further detailed information on the study sites can be found in Marsh et al. (2012) and Rogers et al. (2012).

Kiwa tyleri, *Vulcanolepas scotiaensis* and *Gigantopelta chessoia* were collected by suction sampler using the ROV 'Isis' and separated into acrylic chambers or perspex boxes by species. No female *K. tyleri* were collected from E9 for stable isotope analysis. E2 *K. tyleri* were sorted into sexes before carapace length was measured. *V. scotianensis* are hermaphrodites so could not be split into separate sexes (Buckeridge et al. 2013). The capitulum length was measured in *V. scotiaensis*. *G. chessoia* were not split into sexes because there is no sexual dimorphism and sex can only be determined by examining whether the gonads contain sperm or eggs (Chen et al. 2015). Shell length was measured along the central axis from the shell apex to the outer lip. Length measurements (mm) were taken for each individual using Vernier callipers on recovery of the specimen. Muscle was removed from the chelipeds of *K. tyleri*, whole *V. scotiaensis* were removed from their shells and the foot was dissected from *G. chessoia*. All samples were rinsed with distilled water, stored in glass vials and frozen at −80°C.

Tissue and whole animal samples were freeze dried and ground to a homogeneous powder using a pestle and mortar. Approximately 0.7 mg of powder was weighed into a tin capsule for carbon and nitrogen stable isotope analysis. Dual stable carbon and nitrogen isotope ratios were measured by continuous-flow isotope ratio mass spectrometry using a Costech Elemental Analyser interfaced with Thermo Finnigan Delta Plus XP (Natural Environment Research Council, Life Sciences Mass Spectrometry Facility, SUERC, East Kilbride, UK). Two laboratory standards were analysed for every 10 samples in each analytical sequence. These alternated between paired alanine standards, differing in $\delta^{13}C$ and $\delta^{15}N$, and an internal laboratory gelatin standard. Stable isotope ratios were expressed in delta (δ) notation as parts per thousand/permil (‰). All internal standards are traceable to the following international standards: VPDB (Vienna Pee Dee Belemnite) for carbon and AIR (atmospheric nitrogen) for nitrogen. Freeze-dried and ground deep-sea fish white muscle *Antimora rostrata* was also analysed ($\delta^{13}C$, n = 24, −18.94‰ ± SD 0.09; $\delta^{15}N$, n = 24, 13.11‰ ± SD 0.38) as an external reference material (Jardine & Cunjak 2005).

Data analysis

Isotopic niches were investigated by examining the dispersion of $\delta^{13}C$ and $\delta^{15}N$ values in *xy*-space by calculating the sample size-corrected SEA (SEAc), the Bayesian SEA (SEAb) and the SEAc parameters *E* and θ in the SIAR package (Parnell et al. 2010) implemented in the R statistical package version 3.0.1 (R Core Development Team 2013). *E* is dictated by variance on the *x*- and *y*-axes: low *E* will have similar variance on each axis, i.e. more circular, while high *E* indicates that the ellipse is stretched along the *x*- or *y*-axis. θ is returned as a value between 0 and pi (Jackson et al. 2011) and is reported here in degrees between 0° and 180° where positive or negative values indicate the inclination of the ellipse. θ values close to 0° or 90° suggest dispersion in only 1 axis: θ values close to 0° represent relative dispersion along

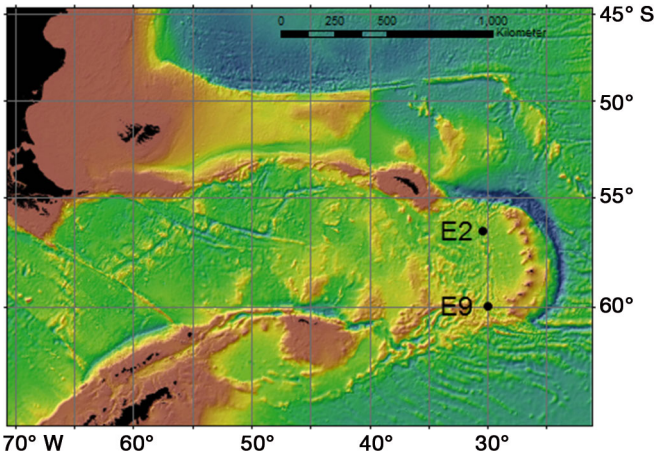

Fig. 1. Bathymetric map indicating the position of the E2 and E9 vent fields on the East Scotia Ridge, Southern Ocean

the *x*-axis ($\delta^{13}C$), indicating utilisation of multiple resources or source mixing, whereas as θ values approach 90°, the ellipse is dispersed along the *y*-axis ($\delta^{15}N$), indicating that individuals within a site are feeding across different trophic positions within a uniform basal source. Further mathematical details for calculating SEA can be found in Jackson et al. (2011).

In order to compare isotopic niche area between sexes or among sites, a Bayesian approach was used that calculated 100 000 posterior iterations of SEAb based on the data set. This produced a range of SEAb probable values, and we report the mode along with 95% credible intervals. Bayesian inference allows a direct probabilistic interpretation of the differences in SEAb depending on the grouping level. This can be achieved through pair-wise comparisons by calculating the proportion of SEAb that differed between 2 groups and can be interpreted as a direct proxy for the probability that one group is larger than the other (Jackson et al. 2011).

Generalised least squares (GLS) regression was used to investigate whether there were site-specific (E2, E9N and E9S) differences in the relationship between $\delta^{13}C$ or $\delta^{15}N$ and length using the nlme R package (Pinheiro et al. 2013). Male and female *K. tyleri* were collected at E2 allowing for a within-site comparison between the sexes. The optimal fixed structure of the model was determined using the relationship between either $\delta^{13}C$ and $\delta^{15}N$ and length and then testing site or sex as an additive or interactive term. Model parameter estimates were initially generated using maximum likelihood (ML) estimation. The Akaike information criteria (AIC) were calculated for each model in order to assess the relative 'goodness-of-fit' using the MuMIn R package (Barton 2014). The model with lowest AIC value was judged to be the best-fitting model unless the difference between AIC (ΔAIC) values was <2. Where ΔAIC is <2, then there is substantial support for both models (Burnham & Anderson 2002). In such circumstances, the most parsimonious model was chosen. Model validation was undertaken by assessing normality and homogeneity of variance of the best-fitting model using: Q-Q plots, histograms of standardised residuals, plots of standardised residuals versus fitted values, and box-plots of standardised residuals per site or sex. Where the assumptions of normality or homogeneity of variance were violated, data were either log transformed or a variance covariance structure was incorporated into the modelling framework. Length was log transformed prior to analysis when examining the $\delta^{15}N$–length relationship for *V. scotiaensis* in order to meet the assumptions of normality. Log transformation was not required for the other 2 species nor for $\delta^{13}C$–length relationship for *V. scotiaensis*. The optimal variance term was then investigated, and subsequent models were fitted using restricted maximum likelihood estimation (REML) and compared using AIC as described above. Once the optimal variance term was found, the model validation process was repeated to check that the underlying assumptions of the GLS were met.

RESULTS

Spatial and sex differences in isotopic niche area

Isotopic niche area ($‰^2$), as delineated by SEAc, for *Kiwa tyleri*, *Vulcanolepas scotiaensis* and *Gigantopelta chessoia* are depicted in Fig. 2A–C. The SEAc for *K. tyleri* ranged from 1.08 $‰^2$ (E9S) to 2.80 $‰^2$ (E2) in male *K. tyleri* while female *K. tyleri* SEAc at E2 was 2.11 $‰^2$ (Table 1). Male and female E2 *K. tyleri* had similar isotopic niche areas (probability = 0.80) based on the distribution of SEAb. Male *K. tyleri* at E2 had a greater isotopic niche than at E9N (probability = 0.98) and E9S (probability = 0.99) (Fig. 2D). Similar isotopic niche areas were also observed in male *K. tyleri* between E9S and E9N (probability = 0.85) (Fig. 2D). *V. scotiaensis* SEAc ranged from 1.07 $‰^2$ (E9N) to 1.55 $‰^2$ (E2). All pair-wise comparisons between sites using SEAb indicated that isotopic niche areas were similar: E9N and E2 (probability = 0.56); E9S and E2 (probability = 0.67); and E9S and E9N (probability = 0.62) (Fig. 2E). The SEAc for *G. chessoia* ranged from 0.69 $‰^2$ (E2) to 1.00 $‰^2$ (E9N) (Table 1) and was lower than the other 2 species. Isotopic niche areas compared by Bayesian inference using SEAb were similar at all sites (Fig. 2F): E2 and E9N (probability = 0.56); E2 and E9S (probability = 0.85); and E9N and E9S (probability = 0.83).

Distinguishing SEAc with *E* and θ

A qualitative assessment of isotopic niche areas using SEAc parameters *E* and θ revealed spatial differences in isotopic niches. *E* was greater in male *K. tyleri* at E9N than E9S, whereas θ indicated a positive relationship between $\delta^{13}C$ and $\delta^{15}N$ at E9N while there was a negative relationship at E9S. At E2, *E*

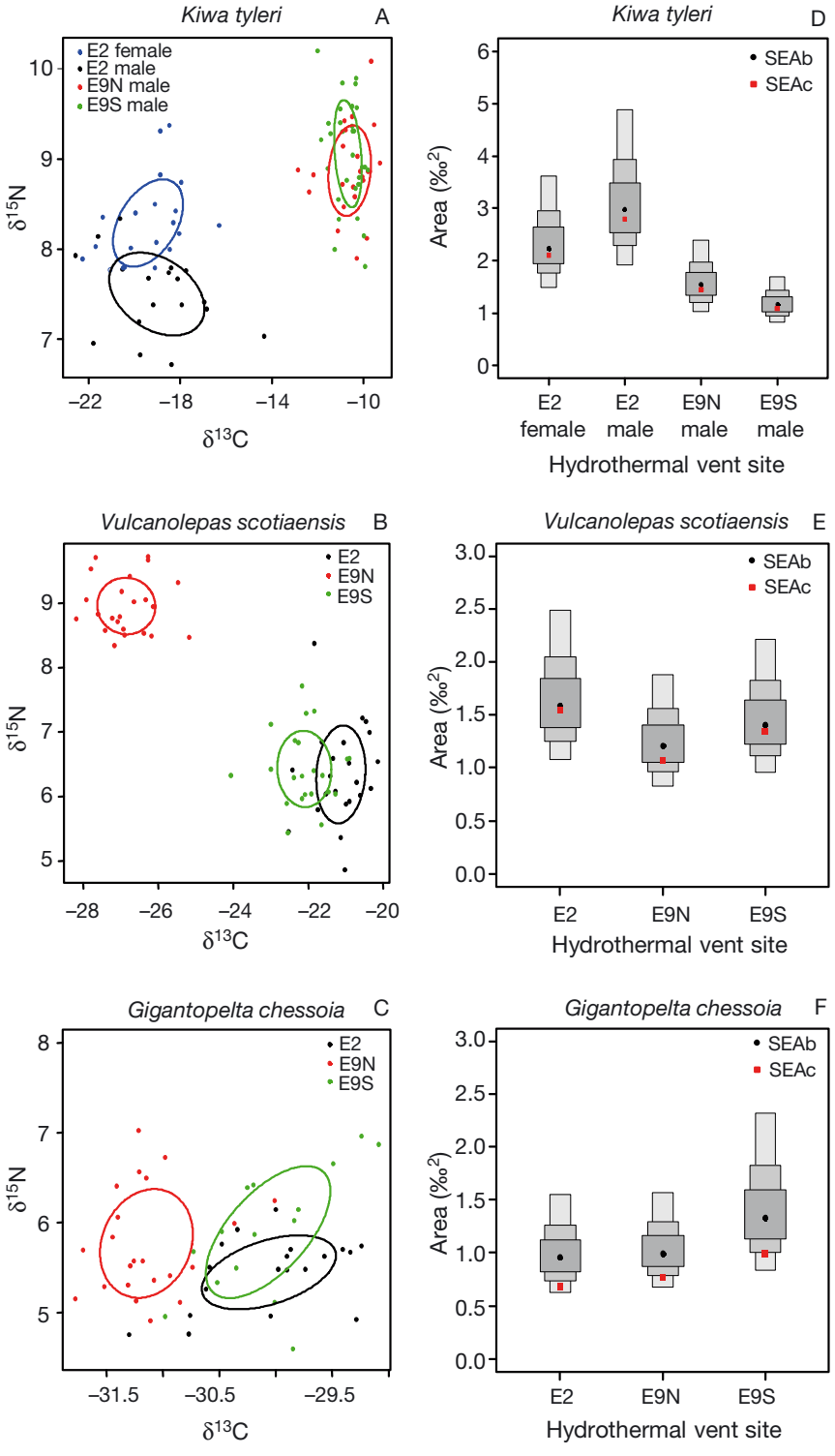

Fig. 2. (A–C) Sample size-corrected standard ellipse area (SEAc) calculated from $\delta^{13}C$ and $\delta^{15}N$ values for *Kiwa tyleri*, *Vulcanolepas scotianesis* and *Gigantopelta chessoia* collected from the East Scotia Ridge (ESR), Southern Ocean, and (D–F) the posterior Bayesian estimates of the standard ellipse area (SEAb). Shaded density plots represent 50, 75 and 95% credible intervals in decreasing order of size, with SEAb mode indicated by a black circle and SEAc by a red square

was similar between female and male *K. tyleri*, whereas θ indicated the relationship between $\delta^{13}C$ and $\delta^{15}N$ was positive for females and negative for males (Table 1, Fig. 2A). In *V. scotiaensis*, both *E* and θ varied among the sites; *E* was similar at E2 and E9S but greater at E9N, while θ at E2 was positive but negative at E9N and E9S (Table 1, Fig. 2B). For *G. chessoia*, *E* indicated that SEAc were similar in shape but θ varied among the sites (Table 1, Fig. 2C).

Spatial and sex differences in $\delta^{13}C$ and $\delta^{15}N$ length-based trends

Evidence of intraspecific variability in $\delta^{13}C$ driven by length was observed in all 3 species (Fig. 3). The GLS indicated that there was a positive relationship between $\delta^{13}C$ and length in male and female *K. tyleri* at E2 (Table 2; Fig. 3A). The length × sex interaction was marginal ($p = 0.08$), which indicated no difference in the slopes. There was a positive relationship between $\delta^{13}C$ and length in male *K. tyleri* that varied by location (Fig. 3B) and included a term that allowed variance to differ by site. Taking E2 as the baseline reference level, the intercepts differed between both E9N and E9S and E2, and there was an interaction between E2 and E9S (Table 2). There was a positive relationship between $\delta^{13}C$ and length for *V. scotiaensis* (Fig. 3C) with the slope similar at each site, but the E9N and E9S intercepts were different to E2 (Table 2). $\delta^{13}C$–length relationships were positive for *G. chessoia* at E2 and E9S while a negative relationship was observed at E9N (Fig. 3D), indicating a length × site interaction (Table 2). The intercept also differed between E2 and E9N (Table 2).

Length was often a covariate describing intraspecific variability in $\delta^{15}N$ (Fig. 4). The optimal GLS model describing the relationship between $\delta^{15}N$ and length for male and female

Table 1. Isotopic niche area (‰^{2}) estimates and parameters (eccentricity [*E*] and the angle between the semi-major axis of the SEAc and the *x*-axis [θ]) for *Kiwa tyleri*, *Gigantopelta chessoia* and *Vulcanolepas scotiaensis* collected from the E2, E9N and E9S vent sites on the East Scotia Ridge (ESR), Southern Ocean. Estimates of isotopic niche areas are given as sample size-corrected standard ellipse area (SEAc) and the mode of the Bayesian standard ellipse area (SEAb) estimates. Upper and lower 95% credible intervals (CI) indicate the uncertainty in the SEAb estimates

Species	n	SEAc	*E*	θ	SEAb	95% CI
Kiwa tyleri						
ESR	90	8.33	0.99	6.47	8.32	6.81 to 10.31
E2 female	20	2.11[a]	0.96	8.31	2.26[a]	1.49 to 3.61[a]
E2 male	18	2.80[a]	0.98	−4.67	2.95[a]	1.92 to 4.88[a]
E9N male	22	1.45	0.85	6.75	1.53	1.03 to 2.39
E9S male	30	1.08	0.68	−43.04	1.16	0.82 to 1.69
Vulcanolepas scotiaensis						
ESR	67	5.79	0.98	−25.31	5.68	4.50 to 7.27
E2	22	1.55	0.55	72.80	1.58	1.07 to 2.49
E9N	23	1.07	0.82	−1.23	1.22	0.82 to 1.88
E9S	22	1.34	0.58	−5.08	1.41	0.95 to 2.21
Gigantopelta chessoia						
ESR	56	1.35	0.65	19.89	1.39	1.07 to 1.82
E2	19	0.69	0.84	24.91	0.96	0.62 to 1.55
E9N	22	0.77	0.75	78.40	1.01	0.67 to 1.57
E9S	15	1.00	0.89	57.58	1.34	0.83 to 2.32

[a]Values from Zwirglmaier et al. (2015)

K. tyleri at E2 (Fig. 4A) included a length × sex interaction and allowed the variance structure to differ by sex. The δ^{15}N–length relationship was negative for males while the relationship was positive for females (Table 3), although the length × sex interaction term was marginal (p = 0.058). The δ^{15}N–length relationship for male *K. tyleri* included a term that allowed the variance to differ by site and with increasing length (Fig. 4B). The δ^{15}N–length relationship was negative at E2 and E9S and positive at E9N (Table 3). In *V. scotiaensis,* δ^{15}N increased with length at E2 and E9S while there was no δ^{15}N–length relationship at E9N (Fig. 4C), which resulted in an interaction between E2 and E9N and differences in the intercept between these 2 areas (Table 3). The optimal GLS model describing the relationship between δ^{15}N and length for the *G. chessoia* had a fixed slope and varying intercepts. The δ^{15}N–length relationship was positive (Fig. 4D) but marginally not significant (p = 0.07); the E9N and E9S intercepts differed from that of E2 (Table 3).

DISCUSSION

The aim here was to examine whether intraspecific spatial variability occurred in isotopic niches and if this was related to sex or body size. All 3 species showed spatial variability in isotopic niche, but this was not necessarily confined to SEAs. There were a number of cases where isotopic niche area compared by Bayesian inference did not differ among sites but *E* and θ provided insight into the difference in the dispersions of δ^{13}C or δ^{15}N. Spatial variation in *E* and θ suggested that there were systematic trends in δ^{13}C and δ^{15}N values for the 3 ESR species studied here and that length was an explanatory variable in several cases.

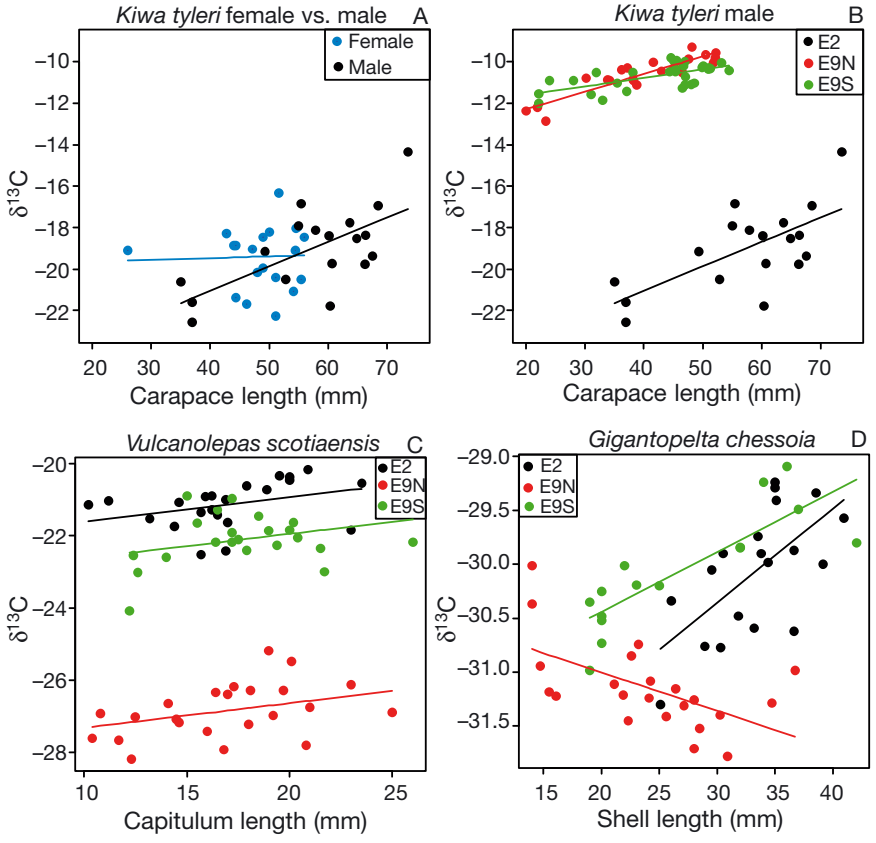

Fig. 3. Relationship between δ^{13}C and length for: (A) male and female *Kiwa* sp. at E2 and (B) male *Kiwa tyleri*, (C) *Vulcanolepas scotianesis*, and (D) *Gigantopelta chessoia* at E2, E9N and E9S. Fitted regression lines were obtained from the generalised least squares models

Table 2. Coefficients for the final $\delta^{13}C$–length generalised least squares models with corresponding standard errors (SE), *t*- and p-values for *Kiwa tyleri*, *Vulcanolepas scotiaensis* and *Gigantopelta chessoia*. Interaction terms are separated by '×' and additive terms by '+'. Coefficients in **bold** represent the reference level for the analysis

Model specification	Coefficients	SE	*t*	p
Kiwa tyleri				
$\delta^{13}C$ = length × sex				
E2 male intercept	**−25.783**	**1.917**	**−13.449**	**<0.001**
E2 male length	**0.118**	**0.032**	**3.595**	**<0.001**
E2 female intercept	6.003	3.183	1.885	0.067
E2 male length × E2 female length	−0.110	0.061	−1.800	0.080
$\delta^{13}C$ = length × site				
E2 male intercept	**−25.783**	**1.917**	**−13.449**	**<0.001**
E2 male length	**0.118**	**0.032**	**3.595**	**<0.001**
E9N male intercept	11.817	1.951	6.056	<0.001
E9S male intercept	13.363	1.956	6.831	<0.001
E2 male length × E9N male length	−0.033	0.034	−0.986	0.327
E2 male length × E9S male length	−0.076	0.034	−2.256	<0.05
Vulcanolepas scotiaensis				
$\delta^{13}C$ = length + site				
E9N intercept	−22.284	0.423	−52.572	**<0.001**
E9N length	0.067	0.023	2.889	**<0.01**
E2 intercept	−5.711	0.198	−28.749	<0.001
E9S intercept	−1.101	0.201	−5.042	<0.001
Gigantopelta chessoia				
$\delta^{13}C$ = length × site				
E2 intercept	**−32.975**	**0.701**	**−46.979**	**<0.001**
E2 length	**0.087**	**0.020**	**4.184**	**<0.001**
E9N intercept	2.687	0.770	3.490	<0.001
E9S intercept	1.418	0.786	1.805	0.077
E2 length × E9N length	−0.123	0.024	−5.030	<0.001
E2 length × E9S length	−0.031	0.024	−1.296	0.200

Differences in isotopic niche area

Isotopic niche area differed among sites for male *Kiwa tyleri,* which may be a related to site-specific differences in epibiont communities that is believed to be their main food source (Reid et al. 2013, Zwirglmaier et al. 2015). The dominant carbon fixation pathway of *Gammaproteobacteria* is the Calvin Benson Bassham (CBB) cycle while *Epsilonproteobacteria* utilise the reductive tricarboxylic acid (rTCA) cycle, which results in the production of organic carbon with different $\delta^{13}C$ values (Hugler & Sievert 2011). The $\delta^{13}C$ values of dissolved inorganic carbon (DIC) at E2 and E9S were ~0.4‰ while at E9N it was 1.5‰ (Reid et al. 2013). This indicates only a minimal difference in the inorganic substrate that would be used for carbon fixation. The resultant $\delta^{13}C$ values of carbon fixed via the rTCA cycle by *Epsilonproteobacteria* would be between −12.6 and −1.6‰ at E2 and E9S and −11.5 and −0.5‰ if isotopic discrimination between $\delta^{13}C$ DIC and microbial biomass was between −13 and −2‰ (House et al. 2003). For *Gammaproteobacteria*, the $\delta^{13}C$ values of microbial biomass would expected to be between −28.6 and −17.6‰ at E2 and E9S, while at E9N the range would be −27.5 to −16.5‰ if isotopic discrimination was between −29 and −18‰ (Robinson & Cavanaugh 1995, Robinson et al. 2003, Scott 2003, Scott et al. 2007). Epibiont diversity at E2 is greater than E9, and the composition also appears to be different with a mix of *Gammaproteobacteria* (50 to 80%) and *Epsilonproteobacteria* (5 to 45%) at E2 compared to a community dominated by *Epsilonproteobacteria* (65 to 98%) at E9 (Zwirglmaier et al. 2015). The intraspecific variability in $\delta^{13}C$ was greater at E2 than the E9 sites, which was likely driven by the differences in microbial community diversity and composition rather than baseline differences in inorganic carbon source.

There were no spatial differences in isotopic niche area for either *Vulcanolepas scotianesis* or *Gigantopelta chessoia* when compared using SEAb. *V. scotianesis* have long, filamentous cirri on which epibiont communities are found. *V. scotianesis* are the least filamentous of the neolepadine stalked barnacles in contrast to species from the Lau Back Arc Basin and Kermadec Arc (Southward & Newman 1998, Suzuki et al. 2009), indicating that they are unlikely to rely on the epibionts growing on their feeding cirri (Buckeridge et al. 2013). Suspended particulate material at hydrothermal vents is a heterogeneous mix of epi-pelagic photosynthetically derived detritus and microbial aggregations that originate either above or below the surface (Levesque et al. 2005, Limén et al. 2007, Sievert & Vetriani 2012), with $\delta^{13}C$ and $\delta^{15}N$ values varying depending on its composition (Levesque et al. 2005, Limén et al. 2007). Behavioural observations of *V. scotianesis* indicate that they are regularly extending their cirri into the water column, which suggests they are suspension feeders and will depend on localised hydrodynamics that supply their food source. The intraspecific isotopic variability potentially reflects individuals filtering different particles from an available pool or the dietary quality of the particles filtered (Lefebvre et al. 2009, Dubois & Colombo 2014, Richoux et al. 2014). In contrast, *G. chessoia* has an enlarged oesophageal gland containing endobionts, which suggest the potential for a host–symbiont relationship (Chen et al. 2015). The relationship is similar to the related scaly-foot gas-

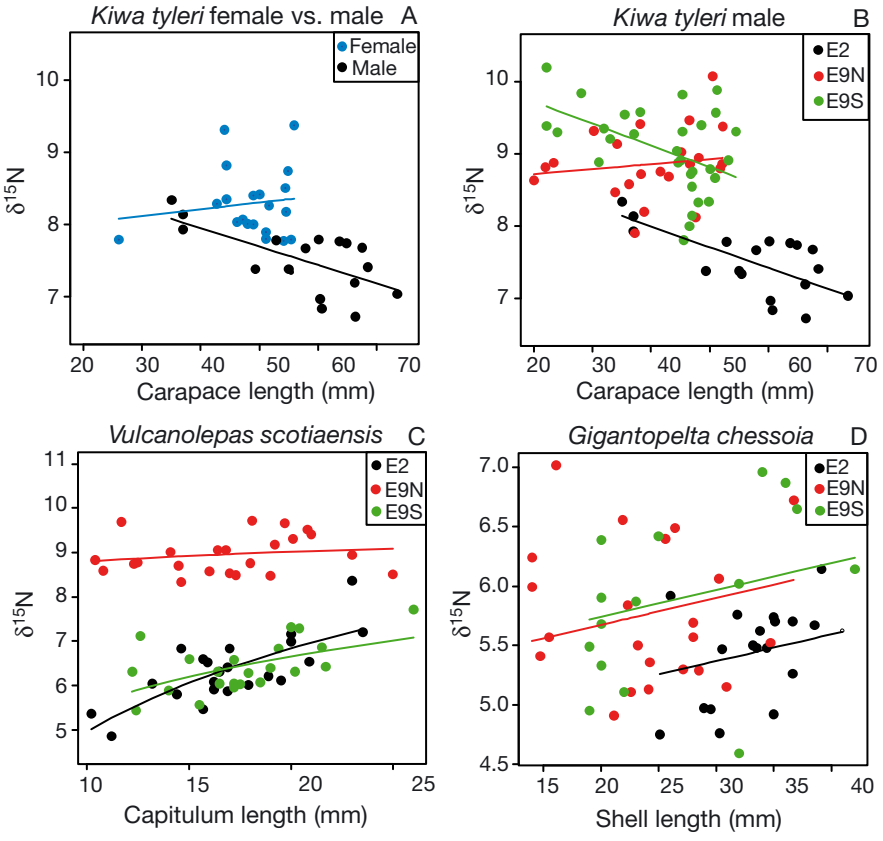

Fig. 4. Relationship between $\delta^{15}N$ and length for: (A) male and female *Kiwa* sp. at E2 and (B) male *Kiwa tyleri*, (C) *Vulcanolepas scotianesis*, and (D) *Gigantopelta chessoia* at E2, E9N and E9S. Fitted regression lines were obtained from the generalised least squares models

tropod (Goffredi et al. 2004). The within-site variability in $\delta^{13}C$ DIC at E2 and E9S is ~1‰, which is similar to the $\delta^{13}C$ variability observed in *G. chessoia*. Therefore, the intraspecific isotopic variability potentially reflects the variation in inorganic substrate isotopic values rather than the consumption of a wide range of food sources. However, for both *V. scotianesis* and *G. chessoia*, physiological factors that can influence isotopic variability at the individual level cannot be ruled out.

Distinguishing SEAc with *E* and θ

Differences in isotopic niches between sexes and among sites could be identified using *E* and θ, and they provided additional information in characterising the isotopic niche rather than just area. The differences were related to the shape and inclination of the SEAc, indicating specific relationships between $\delta^{13}C$ and $\delta^{15}N$. *K. tyleri* males and females from E2 had similar isotopic niche areas, but the inclination of the SEAc differed between sexes. *E* was >0.96, indicating an elongated ellipse and θ being close to 0 indicated that the SEAc was being heavily influenced by $\delta^{13}C$. θ was positive for females and negative for males, which indicated that $\delta^{13}C$ and $\delta^{15}N$ covaried in females, but in males, as $\delta^{13}C$ increased, $\delta^{15}N$ decreased. *V. scotianesis* all had very similar SEAc, and the Bayesian analysis did not show a difference among sites. *E* values at E2 and E9S were different from those at E9N, which indicated that there were differences in the shape of the SEAc. θ indicated that there were site-specific differences in the relationship between $\delta^{13}C$ and $\delta^{15}N$ for *G. chessoia*. θ at E2 was 24.91°, while at E9N it was 78.40°. This indicated that the E2 ellipse was stretched along the *x*-axis, while at E9N the ellipse was less influenced by the *x*-axis but more by the *y*-axis. The differences in θ can be interpreted as $\delta^{13}C$ having a greater influence on the shape of the ellipse at E2 than E9N. Thus, the differences in isotopic variability in the 3 species, at the site or sex level, were revealed by examining *E* and θ; this potentially could result in differences in habitat utilisation, body size or inherent properties of the individual (e.g. specialisation or physiology).

Spatial and sex stable isotope–length relationships

The length-based trends in $\delta^{13}C$ and $\delta^{15}N$ explained part of the isotopic variability in *K. tyleri* SEAc and were also reflected in *E* and θ. The variability in $\delta^{13}C$ and $\delta^{15}N$ defined by both SEAc and *E* was similar for male and female *K. tyleri* at E2. However, θ suggested that there were differences in the way $\delta^{13}C$ and $\delta^{15}N$ values covaried. The negative values of θ in E2 *K. tyleri* male may be explained by an increase in $\delta^{13}C$ and a decrease in $\delta^{15}N$ with length, whereas the positive values of θ in females may have resulted from both $\delta^{13}C$ and $\delta^{15}N$ increasing with length. This resulted in $\delta^{13}C$ and $\delta^{15}N$ values being similar in smaller individuals, but males had lower $\delta^{15}N$ values at larger sizes than females. The differences in the direction of θ may indicate a divergence in habitat use between the sexes and with increasing

Table 3. Coefficients for the final $\delta^{15}N$–length generalised least squares models with corresponding standard errors (SE), *t*- and p-values for *Kiwa tyleri*, *Vulcanolepas scotiaensis* and *Gigantopelta chessoia*. Interaction terms are separated by the symbol '×' and additive terms by '+'. Coefficients in **bold** represent the reference level for the analysis

Model specification	Coefficients	SE	*t*	p
Kiwa tyleri				
$\delta^{15}N$ = length × sex				
E2 male intercept	**8.972**	**0.432**	**20.733**	**<0.001**
E2 male length	**−0.025**	**0.007**	**−3.456**	**<0.01**
E2 female intercept	−1.136	0.908	−1.250	0.219
E2 male length × E2 female length	0.034	0.017	1.955	0.058
$\delta^{15}N$ = length × site				
E2 male intercept	**9.139**	**0.300**	**29.790**	**<0.001**
E2 male length	**−0.028**	**0.005**	**−4.908**	**<0.001**
E9N male intercept	−0.557	0.459	−1.212	0.229
E9S male intercept	0.191	0.454	2.619	<0.01
E2 male length × E9N male length	0.035	0.010	3.249	<0.01
E2 male length × E9S male length	−0.001	0.010	−0.155	0.876
Vulcanolepas scotiaensis				
$\delta^{15}N$ = log(length) × site				
E2 intercept	**−1.254**	**1.430**	**−0.876**	**0.384**
E2 log(length)	**2.699**	**0.507**	**5.322**	**<0.001**
E9N intercept	9.314	1.865	4.992	<0.001
E9S intercept	3.120	2.100	1.480	0.143
E2 log(length) × E9N log(length)	−2.380	0.662	−3.594	<0.001
E2 log(length) × E9S log(length)	−1.100	0.741	−1.483	0.143
Gigantopelta chessoia				
$\delta^{15}N$ = length + site				
E2 intercept	**4.688**	**0.427**	**10.962**	**<0.001**
E2 length	**0.022**	**0.012**	**1.849**	**0.070**
E9N intercept	0.598	0.208	2.867	<0.01
E9S intercept	0.531	0.207	2.556	<0.05

size (Marsh et al. 2012, 2015). The inclination of the SEAc was determined by $\delta^{15}N$ variability, which may be the result of a shifting isotopic baseline. The larger male *K. tyleri* are found close to active venting on chimneys and in areas of elevated diffuse flow while females mainly occur in diffuse flow areas adjacent to the chimneys (Marsh et al. 2012, 2015). The difference in $\delta^{15}N$ may have occurred as a result of different inorganic nitrogen sources as these are not uniform within vents (Johnson et al. 1988). Yet $\delta^{15}N$ values of nitrate and ammonium can be highly variable in diffuse flow fluids and are not necessarily related to temperature (Bourbonnais et al. 2012). Furthermore, the relationship between nitrogen trophic discrimination ($\Delta^{15}N$) and increasing temperature can be negative (Power et al. 2003). Therefore, if the inorganic nitrogen source remains the same, then the negative relationship between size and $\delta^{15}N$ in *K. tyleri* may have been caused by a decrease in $\Delta^{15}N$ between inorganic source and its epibionts, a decrease in $\Delta^{15}N$ between its epibionts and *K. tyleri* or a combination of both.

The spatial analysis of the male *K. tyleri* $\delta^{13}C$– and $\delta^{15}N$–length based trends indicated that there were length × site interactions. θ was negative at E2 and E9S and positive at E9N, which suggested that the relationship between $\delta^{13}C$ and $\delta^{15}N$ varied spatially, which was in accord with the interaction term in the GLS model. At all 3 locations $\delta^{13}C$ increased with length, but a positive $\delta^{15}N$–length relationship only occurred at E9N. The GLS model describing the $\delta^{13}C$–length trend required a variance term because of the greater spread in residuals observed at E2 than E9. This added further support that the larger SEAc in *K. tyleri* at E2 compared to E9 was the result of greater variability in $\delta^{13}C$. The positive $\delta^{13}C$–length relationships were likely to result from changes in *K. tyleri* food source. The epibiont community associated with *K. tyleri* shows great variability, but systemic shifts in the epibiont community with increasing size have not been clearly shown, although small individuals appear to have a greater proportion of *Gammaproteobacteria* than large individuals (Zwirglmaier et al. 2015). In *Rimicaris exoculata*, which occupies a similar ecological niche to *K. tyleri*, there is a shift with size from a *Gammaproteobacteria*-dominated community to one dominated by *Epsilonproteobacteria* (Guri et al. 2012). However, the low sample size in the *K. tyleri* epibiont study may have resulted in the inability to detect a shift in the epibiont community, but the $\delta^{13}C$ data suggested organic carbon fixed by rTCA cycle provided a greater proportion of the diet in large individuals (Zwirglmaier et al. 2015).

Spatial variation in the $\delta^{13}C$– and $\delta^{15}N$–length-based trends indicated there were differences in the trophic ecology of *V. scotianesis* among sites, with variation in θ values reflected in the relationship between $\delta^{13}C$ and $\delta^{15}N$. This was confirmed with the GLS model that described the $\delta^{15}N$–length relationship, which included a length × site interaction term. The cause of the size-based trends are unclear. The closely related stalked barnacle *Leucolepas longa* collects a range of particles from the water column (Tunnicliffe & Southward 2004); as individuals grow, they may have the potential to filter large particles, which are microbially enriched in ^{13}C and ^{15}N relative to small particles as a result of microbial processes (Hoch et al. 1996). However, the structure of barnacles' feeding appendages mean they are not

capable of sorting particles from the water column. Barnacles are dependent on the particles being transported to them that may vary in terms of food quality, which is similar to other marine habitats (Levesque et al. 2005, Dubois & Colombo 2014, Richoux et al. 2014). In the case of $\delta^{15}N$, insufficient protein within the diet (Adams & Sterner 2000) can result in lower growth rates, higher nitrogen turnover rates in the consumer's tissue and increasing $\Delta^{15}N$ (Martinez del Rio et al. 2009). Spatial differences in growth rates as a result of variation in prevailing environmental conditions are proposed in stalked barnacles at volcanic seamounts (Tunnicliffe & Southward 2004). If the *V. scotianesis* diet became deficient in protein with increasing length at E2 or E9S, then $\Delta^{15}N$ may increase in large individuals resulting in the length-based trends in $\delta^{15}N$.

Length-based trends in $\delta^{13}C$ and $\delta^{15}N$ were observed in the *G. chessoia*. θ indicated there were differences in the relationship between $\delta^{13}C$ and $\delta^{15}N$ at each site. The increase in θ from E2 to E9S to E9N matched the change in the slope of the length-based $\delta^{13}C$ trends. However, the mechanism by which these size-based trends occurred was unclear. There are length-based trends in $\delta^{13}C$ and $\delta^{15}N$ of endosymbiont hosting invertebrates at Mid-Atlantic Ridge and East Pacific Rise vent sites (Fisher et al. 1990, Trask & Van Dover 1999, De Busserolles et al. 2009). The mussel *Bathymodiolus azoricus* from the Mid-Atlantic Ridge increases in $\delta^{13}C$ and $\delta^{15}N$ values with length, as a result of differences in the proportions of methane- and sulphur-oxidising bacteria within its gills (Trask & Van Dover 1999, De Busserolles et al. 2009). The length-based trends in *G. chessoia* may be a result of eco-physiological influences on trophic discrimination by the endosymbiont. Eco-physiological influences on endosymbiont could occur through CO_2 limitation in the endosymbionts (Fisher et al. 1990) or increasing diffusion distance for CO_2 travelling from the environment through the host tissue to the endosymbionts (Trask & Van Dover 1999, Scott 2003). Increases in microbial cell density can affect isotopic discrimination because microbes deplete substrate around the cell (Kampara et al. 2009). If endosymbiont density changes with size, then this may be reflected in the stable isotope values of the host tissue. Further explanations include the accumulation of the heavier isotope (^{13}C and ^{15}N) in the tissue over time (Trask & Van Dover 1999), attributable to an increase in the volume of structural tissue (Emmery et al. 2011). However, these explanations all suggest an increase in $\delta^{13}C$ with length, whereas at E9N *G. chessoia* $\delta^{13}C$ decreased with length.

CONCLUSIONS

SEAc and their parameters in conjunction with length-based analyses described some of the isotopic variability within each species. In *Kiwa tyleri* and *Gigantopelta chessoia* a link between *E* and θ was observed that reflected the length-based $\delta^{13}C$ and $\delta^{15}N$ trends. *E* and θ, thus, have the potential to identify if pairs of stable isotope values are related. At present, *E* and θ only provided a qualitative assessment of differences among SEAc as there is no Bayesian approach to assessing the probability that *E* or θ differ among sites. Incorporating these into the statistical analysis would expand the options for testing differences among SEAs but also provide further insight into what is potentially driving the isotopic variability. A better understanding of how *E* and θ interact when *E* becomes more circular ($E \rightarrow 0$) is also required. It may be that as *E* becomes more circular, θ is more difficult to interpret. Further work is needed to understand and refine the use of *E* and θ in ecological studies.

Acknowledgements. The authors thank the officers, technical staff, ROV 'Isis' staff and scientists on board the research cruise JC42 for all their assistance as well as Dr. Andrew Close for providing advice on the generalised least squares analysis. The work was funded by the Natural Environment Research Council: consisting of the studentship NE/F010664/1; ChEsSO consortium grant NE/D01249X/1; and Life Science Mass Spectrometry Facility grant LSMF-BRIS043_04/10_R_09/10.

LITERATURE CITED

Adams TS, Sterner RW (2000) The effect of dietary nitrogen content on trophic level ^{15}N enrichment. Limnol Oceanogr 45:601–607

Barton K (2014) MuMIn: Multi-model inference. http://CRAN.R-project.org/package=MuMIn

Bearhop S, Adams CE, Waldron S, Fuller RA, Macleod H (2004) Determining trophic niche width: a novel approach using stable isotope analysis. J Anim Ecol 73: 1007–1012

Bolnick DI, Svanback R, Fordyce JA, Yang LH, Davis JM, Hulsey CD, Forister ML (2003) The ecology of individuals: incidence and implications of individual specialization. Am Nat 161:1–28

Bourbonnais A, Lehmann MF, Butterfield DA, Juniper SK (2012) Subseafloor nitrogen transformations in diffuse hydrothermal vent fluids of the Juan de Fuca Ridge evidenced by the isotopic composition of nitrate and ammonium. Geochem Geophys Geosyst 13:Q02T01, doi: 10.1029/2011GC003863

Buckeridge JS, Linse K, Jackson JA (2013) *Vulcanolepas scotiaensis* sp nov., a new deep-sea scalpelliform barnacle (Eolepadidae: Neolepadinae) from hydrothermal vents in the Scotia Sea, Antarctica. Zootaxa 3745:551–568

Burnham KP, Anderson DR (2002) Model selection and multimodel inference: a practical information-theoretic approach. Springer, New York, NY

Caut S, Angulo E, Courchamp F (2009) Variation in discrimination factors ($\delta^{15}N$ and $\delta^{13}C$): the effect of diet isotopic values and applications for diet reconstruction. J Appl Ecol 46:443–453

Chen C, Linse K, Roterman CN, Copley JT, Rogers AD (2015) A new genus of large hydrothermal vent-endemic gastropod (Neophalina: Peltospiridae). Zool J Linn Soc 175:319–335

Colaco A, Dehairs F, Desbruyeres D (2002) Nutritional relations of deep-sea hydrothermal fields at the Mid-Atlantic Ridge: a stable isotope approach. Deep-Sea Res I 49:395–412

De Busserolles F, Sarrazin J, Gauthier O, Gelinas Y, Fabri MC, Sarradin PM, Desbruyeres D (2009) Are spatial variations in the diets of hydrothermal fauna linked to local environmental conditions? Deep-Sea Res II 56: 1649–1664

Deudero S, Box A, Vazquez-Luis M, Arroyo NL (2014) Benthic community responses to macroalgae invasions in seagrass beds: diversity, isotopic niche and food web structure at community level. Estuar Coast Shelf Sci 142: 12–22

Dubois SF, Colombo F (2014) How picky can you be? Temporal variations in trophic niches of co-occurring suspension-feeding species. Food Webs 1:1–9

Emmery A, Lefebvre S, Alunno-Bruscia M, Kooijman S (2011) Understanding the dynamics of $\delta^{13}C$ and $\delta^{15}N$ in soft tissues of the bivalve *Crassostrea gigas* facing environmental fluctuations in the context of Dynamic Energy Budgets (DEB). J Sea Res 66:361–371

Fisher CR, Kennicutt MC, Brooks JM (1990) Stable carbon isotopic evidence for carbon limitation in hydrothermal vent vestimentiferans. Science 247:1094–1096

Forero MG, Hobson KA, Bortolotti GR, Donázar JA, Bertellotti M, Blanco G (2002) Food resource utilisation by the Magellanic penguin evaluated through stable-isotope analysis: segregation by sex and age and influence on offspring quality. Mar Ecol Prog Ser 234:289–299

Goffredi SK, Waren A, Orphan VJ, Van Dover CL, Vrijenhoek RC (2004) Novel forms of structural integration between microbes and a hydrothermal vent gastropod from the Indian Ocean. Appl Environ Microbiol 70: 3082–3090

Guri M, Durand L, Cueff-Gauchard V, Zbinden M, Crassous P, Shillito B, Cambon-Bonavita MA (2012) Acquisition of epibiotic bacteria along the life cycle of the hydrothermal shrimp *Rimicaris exoculata*. ISME J 6:597–609

Hesslein RH, Hallard KA, Ramlal P (1993) Replacement of sulfur, carbon, and nitrogen in tissue of growing broad whitefish (*Coregonus nasus*) in response to a change in diet traced by $\delta^{34}S$, $\delta^{13}C$ and $\delta^{15}N$. Can J Fish Aquat Sci 50:2071–2076

Hoch MP, Snyder RA, Cifuentes LA, Coffin RB (1996) Stable isotope dynamics of nitrogen recycled during interactions among marine bacteria and protists. Mar Ecol Prog Ser 132:229–239

House CH, Schopf JW, Stetter KO (2003) Carbon isotopic fractionation by archaeans and other thermophilic prokaryotes. Org Geochem 34:345–356

Hügler M, Sievert SM (2011) Beyond the Calvin cycle: autotrophic carbon fixation in the ocean. Annu Rev Mar Sci 3: 261–289

Hutchinson GE (1957) Concluding remarks. Cold Spring Harbour Symp Quan Biol 22:415–427

Jackson AL, Inger R, Parnell AC, Bearhop S (2011) Comparing isotopic niche widths among and within communities: SIBER –stable isotope Bayesian ellipses in R. J Anim Ecol 80:595–602

James RH, Green DRH, Stock MJ, Alker BJ and others (2014) Composition of hydrothermal fluids and mineralogy of associated chimney material on the East Scotia Ridge back-arc spreading centre. Geochim Cosmochim Acta 139:47–71

Jardine TD, Cunjak RA (2005) Analytical error in stable isotope ecology. Oecologia 144:528–533

Johnson KS, Childress JJ, Hessler RR, Sakamotoarnold CM (1988) Chemical and biological interactions in the Rose Garden hydrothermal vent field, Galapagos Spreading Center. Deep-Sea Res A 35:1723–1744

Kampara M, Thullner M, Harms H, Wick LY (2009) Impact of cell density on microbially induced stable isotope fractionation. Appl Microbiol Biotechnol 81:977–985

Layman CA, Arrington DA, Montana CG, Post DM (2007a) Can stable isotope ratios provide for community-wide measures of trophic structure? Ecology 88:42–48

Layman CA, Quattrochi JP, Peyer CM, Allgeier JE (2007b) Niche width collapse in a resilient top predator following ecosystem fragmentation. Ecol Lett 10:937–944

Layman CA, Araujo MS, Boucek R, Hammerschlag-Peyer CM and others (2012) Applying stable isotopes to examine food-web structure: an overview of analytical tools. Biol Rev Camb Philos Soc 87:545–562

Lefebvre S, Leal JCM, Dubois S, Orvain F and others (2009) Seasonal dynamics of trophic relationships among co-occurring suspension-feeders in two shellfish culture dominated ecosystems. Estuar Coast Shelf Sci 82: 415–425

Levesque C, Limén H, Juniper SK (2005) Origin, composition and nutritional quality of particulate matter at deep-sea hydrothermal vents on Axial Volcano, NE Pacific. Mar Ecol Prog Ser 289:43–52

Limén H, Levesque C, Juniper SK (2007) POM in macro-/meiofaunal food webs associated with three flow regimes at deep-sea hydrothermal vents on Axial Volcano, Juan de Fuca Ridge. Mar Biol 153:129–139

Marsh L, Copley JT, Huvenne VAI, Linse K and others (2012) Microdistribution of faunal assemblages at deep-sea hydrothermal vents in the Southern Ocean. PLoS ONE 7:e48348

Marsh L, Copley JT, Tyler PA, Thatje S (2015) In hot and cold water: differential life-history traits are key to success in contrasting thermal deep-sea environments. J Anim Ecol 84:898–913

Martinez del Rio C, Wolf N, Carleton SA, Gannes LZ (2009) Isotopic ecology ten years after a call for more laboratory experiments. Biol Rev Camb Philos Soc 84:91–111

McMahon KW, Hamady LL, Thorrold SR (2013) A review of ecogeochemistry approaches to estimating movements of marine animals. Limnol Oceanogr 58:697–714

Newsome SD, Martinez del Rio C, Bearhop S, Phillips DL (2007) A niche for isotopic ecology. Front Ecol Environ 5: 429–436

Parnell AC, Jackson AL (2011) SIAR: stable isotope analysis in R. http://CRAN.R-project.org/package=siar

Parnell AC, Inger R, Bearhop S, Jackson AL (2010) Source partitioning using stable isotopes: coping with too much variation. PLoS ONE 5:e9672

Peterson AT, Soberon J, Pearson RG, Anderson RP, Martinez-Meyer E, Nakamura M, Araujo MB (2011) Ecoloigical niches and geographic distribution. Princeton University Press, Oxford

Pinheiro J, Bates D, DebRoy S, Sarker D, Team RDC (2013) nlme: linear and nonlinear mixed effects models. http://CRAN.R-project.org/package=nlme

Pinnegar JK, Polunin NVC (1999) Differential fractionation of $\delta^{13}C$ and $\delta^{15}N$ among fish tissues: implications for the study of trophic interactions. Funct Ecol 13:225–231

Podowski EL, Ma SF, Luther GW, Wardrop D, Fisher CR (2010) Biotic and abiotic factors affecting distributions of megafauna in diffuse flow on andesite and basalt along the Eastern Lau Spreading Center, Tonga. Mar Ecol Prog Ser 418:25–45

Post DM (2002) The long and short of food-chain length. Trends Ecol Evol 17:269–277

Power M, Guiguer K, Barton DR (2003) Effects of temperature on isotopic enrichment in *Daphnia magna*: implications for aquatic food-web studies. Rapid Commun Mass Spectrom 17:1619–1625

R Core Development Team (2013) R: a language and environment for statistical computing. R Foundation for Statistical Computing, Vienna

Ramirez-Llodra E, Tyler PA, Copley JTP (2000) Reproductive biology of three caridean shrimp, *Rimicaris exoculata, Chorocaris chacei* and *Mirocaris fortunata* (Carudea: Decapoda), from hydrothermal vents. J Mar Biol Assoc UK 80:473–484

Reid WDK, Sweeting CJ, Wigham BD, Zwirglmaier K and others (2013) Spatial differences in East Scotia Ridge hydrothermal vent food webs: influences of chemistry, micorbiology and predation on trophodynamics. PLoS ONE 8:e65553

Richoux NB, Vermeulen I, Froneman PW (2014) Stable isotope ratios indicate differential omnivory among syntopic rocky shore suspension-feeders. Mar Biol 161:971–984

Robinson JL, Cavanaugh CM (1995) Rubisco in chemoautotrophic symbioses: implications for the interpretation of stable carbon isotope values. Limnol Oceanogr 40: 1496–1502

Robinson JJ, Scott KM, Swanson ST, O'Leary MH, Horken K, Tabita FR, Cavanaugh CM (2003) Kinetic isotope effect and characterization of form II RubisCO from the chemoautotrophic endosymbionts of the hydrothermal vent tubeworm *Riftia pachyptila*. Limnol Oceanogr 48: 48–54

Rogers AD, Tyler PA, Connelly DP, Copley JT and others (2012) The discovery of new deep-sea hydrothermal vent communities in the Southern Ocean and implications for biogeography. PLoS Biol 10:e1001234

Scott KM (2003) A $\delta^{13}C$-based carbon flux model for the hydrothermal vent chemoautotrophic symbiosis *Riftia pachyptila* predicts sizeable CO_2 gradients at the host–symbiont interface. Environ Microbiol 5:424–432

Scott KM, Henn-Sax M, Harmer TL, Longo DL, Frame CH, Cavanaugh CM (2007) Kinetic isotope effect and biochemical characterization of form IA RubisCO from the marine cyanobacterium *Prochlorococcus marinus* MIT9313. Limnol Oceanogr 52:2199–2204

Sievert SM, Vetriani C (2012) Chemoautotrophy at deep-sea vents past, present, and future. Oceanography (Wash DC) 25:218–233

Southward AJ, Newman WA (1998) Ectosymbiosis between filamentous sulphur bacteria and a stalked barnacle (Scalpellomorpha, Neolepadinae) from the Lau Back Arc Basin, Tonga. Cah Biol Mar 39:259–262

Suzuki Y, Suzuki M, Tsuchida S, Takai K and others (2009) Molecular investigations of the stalked barnacle *Vulcanolepas osheai* and the epibiotic bacteria from the Brothers Caldera, Kermadec Arc, New Zealand. J Mar Biol Assoc UK 89:727–733

Sweeting CJ, Jennings S, Polunin NVC (2005) Variance in isotopic signatures as a descriptor of tissue turnover and degree of omnivory. Funct Ecol 19:777–784

Syväranta J, Lensu A, Marjomaki TJ, Oksanen S, Jones RI (2013) An empirical evaluation of the utility of convex hull and standard ellipse areas for assessing population niche widths from stable isotope data. PLoS ONE 8: e56094

Thatje S, Marsh L, Roterman CN, Mavrogordato M, Linse K (2015) Adaptations to hydrothermal vent life in *Kiwa tyleri*, a new species of yeti crab from the East Scotia Ridge, Antarctica. PLoS ONE 10:e0127621

Trask JL, Van Dover CL (1999) Site-specific and ontogenetic variations in nutrition of mussels (*Bathymodiolus* sp.) from the Lucky Strike hydrothermal vent field, Mid-Atlantic Ridge. Limnol Oceanogr 44:334–343

Tunnicliffe V, Southward AJ (2004) Growth and breeding of a primitive stalked barnacle *Leucolepas longa* (Cirripedia: Scalpellomorpha: Eolepadidae: Neolepadinae) inhabiting a volcanic seamount off Papua New Guinea. J Mar Biol Assoc UK 84:121–132

Turner TF, Collyer ML, Krabbenhoft TJ (2010) A general hypothesis-testing framework for stable isotope ratios in ecological studies. Ecology 91:2227–2233

Werner EE, Gilliam JF (1984) The ontogenetic niche and species interactions in size-structured populaitons. Annu Rev Ecol Syst 15:393–425

Wiens JJ, Graham CH (2005) Niche conservatism: integrating evolution, ecology, and conservation biology. Annu Rev Ecol Syst 36:519–539

Zwirglmaier K, Reid WDK, Heywood J, Sweeting CJ and others (2015) Linking regional variation of epibiotic bacterial diversity and trophic ecology in a new species of Kiwaidae (Decapoda, Anomura) from East Scotia Ridge (Antarctica) hydrothermal vents. MicrobiologyOpen 4: 136–150

Editorial responsibility: Antonio Bode, A Coruña, Spain

Submitted: May 27, 2015; Accepted: November 24, 2015
Proofs received from author(s): January 8, 2016